First-principles study of spontaneous polarization in multiferroic BiFeO$_3$

J. B. Neaton,[1,*] C. Ederer,[2] U. V. Waghmare,[3] N. A. Spaldin,[2] and K. M. Rabe[1]

[1]*Department of Physics and Astronomy, Rutgers University, Piscataway, New Jersey 08854-8019, USA*
[2]*Materials Research Laboratory and Materials Department, University of California, Santa Barbara, California 93106, USA*
[3]*Jawaharlal Nehru Center for Advanced Scientific Research, Jakkur, Bangalore 560 064, India*

The ground-state structural and electronic properties of ferroelectric BiFeO$_3$ are calculated using density functional theory within the local spin-density approximation (LSDA) and the LSDA$+U$ method. The crystal structure is computed to be rhombohedral with space group $R3c$, and the electronic structure is found to be insulating and antiferromagnetic, both in excellent agreement with available experiments. A large ferroelectric polarization of $90-100$ μC/cm^2 is predicted, consistent with the large atomic displacements in the ferroelectric phase and with recent experimental reports, but differing by an order of magnitude from early experiments. One possible explanation is that the latter may have suffered from large leakage currents. However, both past and contemporary measurements are shown to be consistent with the modern theory of polarization, suggesting that the range of reported polarizations may instead correspond to distinct switching paths in structural space. Modern measurements on well-characterized bulk samples are required to confirm this interpretation.

PACS number(s): 77.80.$-$e, 77.84.$-$s, 77.22.Ej, 71.20.$-$b

I. INTRODUCTION

There has been considerable recent interest in developing multifunctional materials in which two or more useful properties are combined in a single compound. Perhaps the most widely studied class of multifunctional materials are the diluted magnetic semiconductors, where interaction between magnetic and electronic degrees of freedom allows both charge and spin to be manipulated by applied homogeneous electric fields.[1] These and other related materials having spin-dependent electronic properties are presently being explored for spintronic applications.[2] However, another class of materials, the so-called multiferroics,[3,4] is also of growing importance. Multiferroic materials have simultaneous ferromagnetic, ferroelectric, and/or ferroelastic ordering. Coupling between the magnetic and ferroelectric order parameters can lead to *magnetoelectric* effects, in which the magnetization can be tuned by an applied electric field and vice versa. Relatively few multiferroics have been identified,[5] and in those that are known, the mechanism underlying their ferroelectricity is often unconventional.[6,7] The purpose of this work is to understand the unusual ferroelectric behavior in multiferroic BiFeO$_3$, which has recently emerged as an especially promising magnetoelectric multiferroic material.[8]

Recently, large ferroelectric polarizations, exceeding those of prototypical ferroelectrics BaTiO$_3$ and PbTiO$_3$, have been reported in high-quality thin films of BiFeO$_3$.[8–10] These sizable polarizations are consistent with the observed large atomic distortions,[11,12] but apparently inconsistent with earlier studies of *bulk* BiFeO$_3$,[13] a difference whose origin is currently under debate. In addition, appreciable magnetizations ($\sim 1\mu_B$ per formula unit), increasing with decreasing film thickness, have been reported,[8] accompanied by substantial magnetoelectric coupling.

Bulk BiFeO$_3$ has long been known to be ferroelectric[13] with a Curie temperature of about 1100 K. The structure of the ferroelectric phase, resolved experimentally using both x-ray and neutron diffraction,[11,12] can be understood as

highly distorted perovskite with rhombohedral symmetry and space group $R3c$. The primitive unit cell, shown in Fig. 1, contains two formula units (ten atoms), arising from counterrotations of neighboring O octahedra about the [111] axis. The $R3c$ symmetry permits the development of a spontaneous polarization along [111], and Bi, Fe, and O are displaced relative to one another along this threefold axis. The largest relative displacements are those of Bi relative to O, consistent with a stereochemically active Bi lone pair.[7] The polar displacements (relative to cubic perovskite) are noticeably extreme when compared with those in nonlone-pair-active perovskite ferroelectrics such as BaTiO$_3$ or KNbO$_3$, but are consistent with those observed in other Bi-based perovskites.[14] The crystal structure of the paraelectric phase has not been conclusively determined.

Surprisingly, given the large atomic displacements relative to the centrosymmetric cubic perovskite structure, and the high ferroelectric Curie temperature, early measurements on bulk single crystals[13] yielded rather small polarizations. Teague *et al.*[13] initially reported a polarization along [111] of just 6.1 μC/cm^2; although these authors state that their hysteresis loops were not saturated, their measurements were
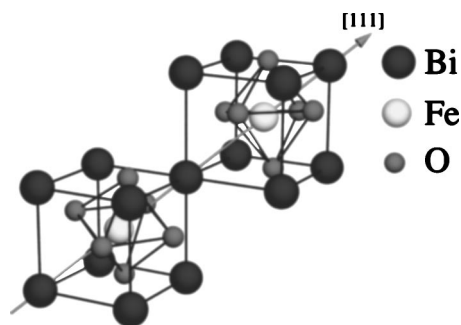

FIG. 1. Structure of $R3c$ BiFeO$_3$. Notice the position of the oxygen octahedra relative to the Bi framework; in the ideal cubic perovskite structure the oxygen ions would occupy the face-centered sites.

TABLE I. Various measured values for the polarization in BiFeO$_3$, in chronological order with the oldest at the top.

Ref.	P (μC/cm^2)	Sample type
13	6.1	Bulk single crystals
15	2.5	(Bi$_{0.7}$Ba$_{0.3}$)(Fe$_{0.7}$Ti$_{0.3}$)O$_3$ films (300 nm) on Nb-doped SrTiO$_3$
16	2.2	Polycrystalline films (200 nm)
8	50–90	Thin films (400–100 nm) on SrRuO$_3$/SrTiO$_3$
18	35.7	Polycrystalline films (350 nm)
17	8.9	Bulk ceramics
10	158	Polycrystalline films (300 nm)

supported by more recent studies of both BiFeO$_3$/BaTiO$_3$ alloy films[15] and pure BiFeO$_3$ polycrystalline films.[16] The small values are in sharp contrast with recent experiments on epitaxial thin film samples of BiFeO$_3$, which were found to possess large polarizations. The first thin film measurements[8] yielded values of 50–90 μC/cm^2 on (100) aligned substrates, increasing to 100 μC/cm^2 for (111) orientations.[9] Following that, a whole variety of different experimental values has been reported[10,17,18] (summarized in Table I), including a very recent report[10] of giant ($>$150 μC/cm^2) polarization, which is the highest value ever measured for a ferroelectric.

There are several plausible explanations for the spread of experimental values. First, the original reports of small polarization might have been limited by poor sample quality, with the large thin film values representing the "true" polarization for $R3c$ BiFeO$_3$. A second possibility is that the small values could be correct for the $R3c$ structure, with the large values being correct for different structural modifications stabilized in the thin films. And finally, a third possibility is that large and small values can be explained within the modern theory of polarization, which recognizes that polarization is in fact a lattice of values, rather than a single vector.[19–21] In this last case, the ferroelectric switching behavior in the different samples would have to be substantially different. In this work, we use first-principles density functional calculations to examine this issue carefully. We find that the most natural value of the polarization is 90–100 μC/cm^2 along the [111] direction, consistent with recent thin film measurements.[8,9] However, both the unexpectedly small early values, and the anomalously large recent values, can be explained within the modern theory of polarization, provided that a suitable switching path can be found.

The remainder of this paper is organized as follows. In Sec. II we describe the *ab initio* methods used throughout this work. In Secs. III A and III B, we report the computed ground-state structural and electronic properties of BiFeO$_3$ and show that they are in good agreement with experiment. In Sec. III C the ferroelectric polarization is calculated using the modern theory of polarization and compared with a simple estimate. In Sec. IV we discuss how the dependence of the polarization on the switching path is a possible explanation for the large spread of reported experimental values.

The intriguing magnetic properties are discussed in a separate study.[22]

II. METHOD

To calculate the structure, polarization, and Born effective charges of BiFeO$_3$, we use density functional theory (DFT) within the local spin-density approximation[23,24] (LSDA) and the LSDA+U method[25] as implemented in the Vienna *ab initio* Simulation Package (VASP).[26,27] All results were obtained using the projector-augmented plane-wave method[28,29] by explicitly treating 15 valence electrons for Bi ($5d^{10}6s^26p^3$), 14 for Fe ($3p^63d^64s^2$), and 6 for oxygen ($2s^22p^4$). Our calculations do not include spin-orbit corrections. Brillouin zone integrations are performed with a Gaussian broadening[30] of 0.1 eV during all relaxations. These calculations are performed with a $3\times3\times3$ Monkhorst–Pack **k**-point mesh[31] centered at Γ and a 500 eV plane-wave cutoff, both of which result in good convergence of the computed ground-state properties.

Since it is well known that the LSDA often underestimates the size of the band gap in systems with strongly localized d orbitals, and even predicts metallic behavior for materials that are known to be insulators,[32] we also calculate the structural and electronic properties within the LSDA+U method.[25] In the LSDA+U framework the strong Coulomb repulsion between localized d states is treated by adding a Hubbard-like term to the effective potential, leading to an improved description of correlation effects in transition-metal oxides. The LSDA+U method requires two parameters, the Hubbard parameter U and the exchange interaction J. Since there is no unique way of including a Hubbard term within the DFT framework, several different approaches exist which all give similar results. In this work we use the approach described by Dudarev *et al.*[33] where only an effective Hubbard parameter $U_{\text{eff}}=U-J$ enters the Hamiltonian. The magnitude of U_{eff} is varied between 0 and 7 eV for the Fe d states (the standard LSDA result corresponds to $U_{\text{eff}}=0$ eV). These calculations are performed with a Γ-centered $5\times5\times5$ Monkhorst-Pack **k**-point mesh and a slightly lower plane-wave cutoff of 400 eV. The tetrahedron method[34] is used for Brillouin zone integrations.

Structural optimizations are performed with both LSDA and LSDA+U energy functionals. The ions are steadily relaxed toward equilibrium until the Hellmann-Feynman forces are less than 10^{-3} eV/Å; other cell parameters are adjusted until stress tensor components are less than 40 meV/cell. Separate optimizations of the $R3c$ phase are performed for U_{eff} values of 0, 2, and 4 eV. Since the LSDA+U method is based on an empirical correction (the Hubbard U) and has been designed chiefly to correct the electronic structure of strongly correlated systems, we mention that it has been rarely used for structural relaxation. Recently, however, the use of U_{eff} has been shown to improve the structural properties of transition-metal sulfides[35] and hematite.[36]

Rock-salt (G-type) antiferromagnetic (AFM) order is assumed for all calculations, as well as a homogeneous and collinear spin arrangement. This assumption is well justified,

TABLE II. Calculated and measured structural parameters of $BiFeO_3$ in space group $R3c$ (point group C_{3v}). The Wyckoff positions $2a$ and $6b$ are referenced to the rhombohedral system and are $Bi(x,x,x)$, $Fe(x,x,x)$, and $O(x,y,z)$. The lattice constant of the rhombohedral primitive cell a_{rh} is given in angstroms, and the rhombohedral angle α and unit cell volume Ω are also provided.

U_{eff} (eV)		0	2	4	Expt. (Ref. 12)
Bi (2a)	x	0	0	0	0
Fe (2a)	x	0.231	0.228	0.227	0.221
O (6b)	x	0.542	0.542	0.542	0.538
	y	0.943	0.942	0.943	0.933
	z	0.398	0.396	0.397	0.395
a_{rh} (Å)		5.46	5.50	5.52	5.63
α (deg)		60.36	59.99	59.84	59.35
Ω (Å^3)		115.98	117.86	118.34	124.60

since in practice $BiFeO_3$ is observed to be nearly G-type AFM. However, experiments also report a long-wavelength spiral spin structure[37] and possibly a small out-of-plane canting due to weak ferromagnetism.[38] Since the noncollinearity is quite minimal, the simplification to a collinear magnetic structure is acceptable. Detailed calculations of the effects of noncollinearity and spin-orbit coupling on the magnetic properties of $BiFeO_3$ appear separately.[22]

The electronic contribution to the polarization is calculated as a Berry phase using the method first developed by King-Smith and Vanderbilt[19,20] (see also Ref. 21), the so-called "modern" theory of polarization. In this approach, the total polarization **P** for a given crystalline geometry can be calculated as the sum of ionic and electronic contributions. The ionic contribution is obtained by summing the product of the position of each ion in the unit cell (with a given choice of basis vectors) with the nominal charge of its rigid core. The electronic contribution to **P** is determined by evaluating the phase of the product of overlaps between cell-periodic Bloch functions along a densely sampled string of neighboring points in **k** space. Here we use four symmetrized strings consisting of 15 **k** points to obtain the electronic contribution to the polarization, which is calculated separately for each spin channel; the total polarization is then the sum of the two spin contributions and the ionic contribution.

III. RESULTS AND DISCUSSION

A. Structure

In Table II we report structural parameters obtained by relaxing the cell volume Ω, rhombohedral angle α, and atomic positions within the $R3c$ space group using the LSDA (i.e., $U_{eff}=0$ eV) and LSDA$+U$ with $U_{eff}=2$ and 4 eV. All sets of parameters are in close agreement with the experimental values of Kubel and Schmid;[12] in particular the internal atomic coordinates are reproduced very well. The lattice constant is underestimated by roughly 3% for $U_{eff}=0$ eV, a large but not atypical consequence of the LSDA. The calcu-

lated and experimental rhombohedral angles are very close to 60° which would correspond to perfectly cubic lattice vectors. The calculated values are slightly larger than experiment for $U_{eff}=0$ eV; we attribute this to the underestimated volume of the LSDA ground state. The effect of U_{eff} on the structural parameters is relatively small, although increasing U_{eff} does tend to improve the agreement with experiment. Given the additional uncertainty introduced by the empirical nature of LSDA$+U$ and the near-negligible quantitative differences for a nonzero U_{eff}, in what follows we use the LSDA structure unless otherwise stated. Our calculations of the total energy for other selected symmetries, including $P4mm$, $R\bar{3}c$, and $R3m$, corroborate $R3c$ as the ground state.

In the ground-state $R3c$ structure, the Bi site is strongly distorted such that only 6 of the 12 oxygens surrounding Bi can still be considered nearest neighbors. For $U_{eff}=0$, three coplanar oxygens lie above Bi along [111] at 2.30 Å, and three sit below at 2.41 Å. Likewise, the Fe site is displaced relative to the center of its surrounding octahedron, which is also distorted, with three oxygen neighbors at 1.92 Å and three others at 2.07 Å. The O—Fe—O bond angle in this system, which would be an ideal 180° in a cubic perovskite structure, buckles to a value of 165°. Indeed $R3c$ $BiFeO_3$ is structurally similar to ferroelectric $LiNbO_3$, which also has $R3c$ symmetry, off-centering of the Li and Nb cations, and large rotations of the oxygen octahedra resulting in a sixfold coordinated site for the large cation.[39,40]

The structural relationship between cubic perovskite and $R3c$ can be understood with just two rather simple distortions from the cubic geometry: (i) counterrotations of adjacent oxygen octahedra *about* [111], and (ii) relative ionic displacements *along* [111]. Freezing in the counterrotations alone results in a nonpolar insulator with $R\bar{3}c$ symmetry, a structural phase of $BiFeO_3$ that, by analogy to $LiNbO_3$, is a possible candidate for its high-temperature paraelectric phase. Freezing in only the polar mode produces a ferroelectric with $R3m$ symmetry.

B. Electronic and magnetic properties

In this section, we present the electronic structure of $BiFeO_3$ computed in the ferroelectric $R3c$ structure. We also briefly discuss results obtained for the cubic perovskite and centrosymmetric $R\bar{3}c$ structures; both are possible paraelectric high-temperature phases.

The single-particle density of states (DOS) for a single spin channel and the DOS of the local Fe d states for both spin channels, calculated within the LSDA, are shown in Figs. 2(a) and 2(b) for $BiFeO_3$ in the $R3c$ structure. Both spin channels exhibit identical total DOSs, as required for an AFM. The structure is insulating, with a small gap of 0.4 eV in the LSDA calculation. This gap is significantly enhanced after application of the LSDA$+U$ method, as seen from Fig. 2(c); for the small value $U_{eff}=2$ eV, the gap is 1.3 eV; for $U_{eff}=4$ eV [Fig. 2(d)] it further increases to 1.9 eV. The narrow bands around the Fermi energy arise predominantly from the Fe $3d$ states (with some oxygen hybridization) and are divided into t_{2g} and e_g manifolds, as expected from their octahedral coordination. Lying below and hybridized with
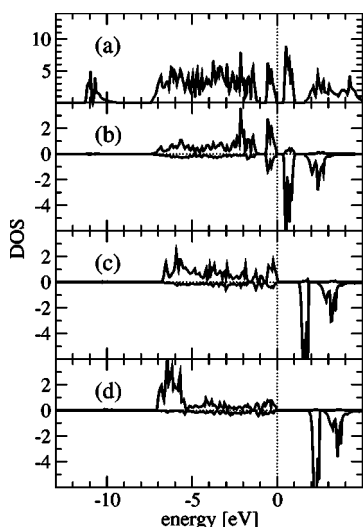
FIG. 2. Calculated densities of states (DOSs) for $R3c$ BiFeO$_3$. Upper panels (a) and (b) show the total DOS for one spin channel and the local Fe DOS for both spin channels (minority spin states are shown as negative) calculated within the LSDA, respectively. Lower panels (c) and (d) show the local Fe DOS obtained from the LSDA+U method with $U_{\mathrm{eff}}=2$ and =4 eV, respectively. The zero is set to the valence band maximum.

the Fe states is the broad predominantly oxygen $2p$ valence band, which also contains a significant amount of Bi $6p$ character. The lowest band shown, at ~ 9.5 eV below the valence band maximum, is the Bi $6s$ band. The large amount of occupied Bi $6p$ states is consistent with the picture of the Bi lone pair as the driving force of the ferroelectric distortion[5,7] in this class of materials.

Figure 3 shows the dispersion of the bands in the energy range around the gap. The band gap is indirect for LSDA ($U_{\mathrm{eff}}=0$ eV) and $U_{\mathrm{eff}}=2$ eV, with the bottom of the conduction band located at the point Z in the rhombohedral Brillouin zone and the top of the valence band between Γ and Z. For a higher value of $U_{\mathrm{eff}}=4$ eV, the gap remains indirect but the top of the valence band shifts to a location between Γ and F. Photoemission spectroscopy would be of use to determine
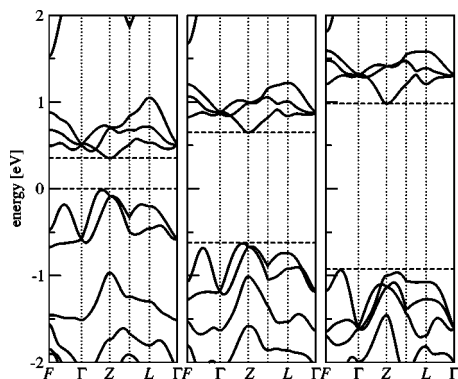

FIG. 3. Band structure of $R3c$ BiFeO$_3$ in the energy region of the gap for $U_{\mathrm{eff}}=0$ (LSDA, left panel), 2 (middle panel), and 4 eV (right panel). The valence and conduction band edges are indicated by the dashed horizontal lines. The high-symmetry **k** points are labeled according to Ref. 41.
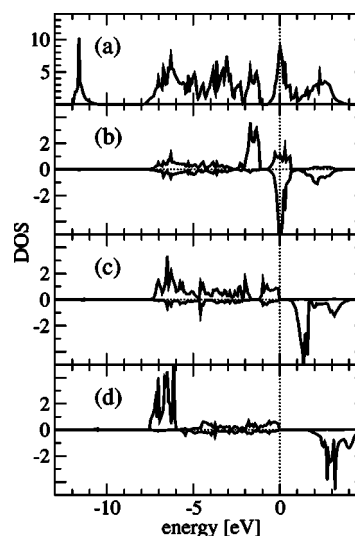

FIG. 4. Calculated densities of states (DOSs) for cubic BiFeO$_3$. Upper panels (a) and (b) show the total DOS for one spin channel, and the local Fe DOS for both spin channels, respectively (minority spin states are shown with a negative sign), both calculated within the LSDA. Lower panels (c) and (d) show the local Fe DOS obtained using the LSDA+U method, with U_{eff} values of 2 and 5 eV. The zero is set to the Fermi energy (a),(b) or valence band maximum (c),(d).

the value of U_{eff} best describing the electronic structure of BiFeO$_3$.

The LSDA local magnetic moment at the Fe atoms (integrated within a sphere of radius 1.4 Å) is $\sim 3.3\mu_{\mathrm{B}}$, in reasonable agreement with the experimental value of $3.75\mu_{\mathrm{B}}$ (Ref. 42). It is reduced from the formal value of $5\mu_{\mathrm{B}}$ for high-spin Fe^{3+} because of the finite bandwidth of the $3d$ states. Use of the LSDA+U method improves the agreement with the experiment, enhancing the Fe magnetic moment to a value of $3.8\mu_{\mathrm{B}}$ for $U_{\mathrm{eff}}=2$ eV and $4.0\mu_{\mathrm{B}}$ for $U_{\mathrm{eff}}=4$ eV.

For comparison, we provide supplementary results for two centrosymmetric phases, the high-symmetry cubic perovskite and rhombohedral $R\bar{3}c$ phases. Both could be considered candidates for the high-temperature paraelectric phase, whose structure is presently unknown; both may also function as reference structures for determining the spontaneous polarization, as will be discussed in Sec. III C. For the cubic perovskite arrangement, a primitive lattice constant of 3.87 Å is used for all calculations and corresponds to a volume per formula unit equal to that of the bulk $R3c$ phase; the unit cell is doubled along [111] to accommodate the opposite spin polarization of the two Fe ions. The single-particle total density of states, calculated within the LSDA, is shown for one spin channel in Fig. 4(a), along with the local density of states for both spin channels on one of the Fe ions [Fig. 4(b)]. Strikingly, BiFeO$_3$ is metallic in this structure within the LSDA, with the Fermi energy cutting through the narrow band composed of up-spin e_g states and down-spin t_{2g} states.

As discussed in Sec. II, the LSDA often fails to describe such narrow d bands correctly. Figures 4(c) and 4(d) show the site-projected local DOS for Fe obtained within the LSDA+U method for two different values of U_{eff}. Including an effective Coulomb repulsion parameter pushes the Fe ma-

TABLE III. Calculated LSDA structural parameters (lattice constant a_{rh}, rhomobohedral angle α, and volume Ω) of $BiFeO_3$ in the space group $R\bar{3}c$ (point group D_{3d}); the Wyckoff positions, referenced to the rhombohedral system, are $(2b)$ Bi$(1/2,1/2,1/2)$, $(2a)$ Fe$(0,0,0)$, and $(6e)$ O$(x,1/2-x,1/4)$.

x	0.417
a_{rh} (Å)	5.35
α (deg)	61.93
Ω (Å³)	113.12

jority d bands down in energy and the Fe minority d bands up, leading to a gap of ~ 0.5 eV for a relatively small U_{eff} of 2 eV. Formation of the fully gapped insulating phase is accompanied by a marked increase in the local Fe magnetic moment from ~ 1.9 to $\sim 3.9 \mu_B$ (suggestive of a crossover from low-spin to high-spin behavior for the Fe ion). Although we predict the cubic perovskite phase of $BiFeO_3$ to be unstable, the fact that such a small U_{eff} (typical values for U_{eff} in other Fe compounds range between $U_{eff}=3$ and 5 eV; Refs. 43 and 44) opens a gap supports the notion that the metallicity is caused primarily by inadequate treatment of strong correlations in LSDA.

Finally, we remark that the centrosymmetric $R\bar{3}c$ structure, mentioned briefly in Sec. III A as a possible candidate paraelectric phase, is already insulating within the LSDA, albeit with a small gap whose magnitude is found to be extremely sensitive to input parameters. As with the cubic perovskite phase, a stable insulating solution can be obtained even for small values of U_{eff}. We perform a full structural relaxation imposing $R\bar{3}c$ symmetry within the LSDA, and the structural parameters resulting from this relaxation are summarized in Table III. Briefly, compared with $R3c$, this arrangement is found to possess a smaller volume and a larger rhombohedral angle. The environment of the A site is drastically changed relative to cubic perovskite: each Bi site has three oxygen neighbors at 2.30 Å, six at 2.71 Å, and three more at 3.21 Å. However, the local octahedral environment of the B site is preserved: each Fe site is octahedrally coordinated with six O neighbors at a distance of 1.97 Å.

C. Spontaneous polarization

1. Estimate using Born effective charges

As discussed above, recent reports of ferroelectric polarizations in high-quality $BiFeO_3$ thin films[8,10] exceed previous measurements on bulk samples[13] by an order of magnitude. The polarizations measured in thin film samples are consistent with the observed large atomic distortions,[11,12] but apparently inconsistent with an earlier study of *bulk* $BiFeO_3$,[13] which reported a modest polarization along [111] of just 6.1 $\mu C/cm^2$.

In an effort to shed light on this issue, we examine the spontaneous polarization **P** of $BiFeO_3$ in its $R3c$ ground state from first principles. Experimentally, **P** corresponds to half the polarization change as the applied field is swept through zero from positive to negative. For prototypical perovskite

TABLE IV. Born effective charges (BECs) for displacements along [111] for $BiFeO_3$ in the cubic perovskite, $R\bar{3}c$, and $R3c$ structures. LSDA+U results are obtained using $U_{eff}=2$ eV. Since cubic perovskite is metallic within the LSDA and the $R\bar{3}c$ structure is nearly so, LSDA values are given only for the $R3c$ structure. ΔP, calculated using Eq. (1) along a path from the cubic structure to $R3c$, is given for each set of BECs.

		LSDA			LSDA+U		
		Bi	Fe	O	Bi	Fe	O
Cubic	Z_j^*				6.32	4.55	−3.06
	ΔP				123.1 $\mu C/cm^2$		
$R\bar{3}c$	Z_j^*				4.92	4.25	−3.06
	ΔP				101.2 $\mu C/cm^2$		
$R3c$	Z_j^*	4.28	3.26	−2.50	4.37	3.49	−2.61
	ΔP	84.2 $\mu C/cm^2$			87.3 $\mu C/cm^2$		

ferroelectrics, it has been standard to estimate this value by simply summing the product of atomic displacements (from a centrosymmetric reference structure) and their corresponding Born effective charges (BECs). This estimate corresponds to computing the Cartesian components of the polarization ΔP_α to linear order in the atomic displacements, i.e.,

$$\Delta P_\alpha \cong \sum_{j\beta} \frac{\partial P_\alpha}{\partial u_{j\beta}}(u_{j\beta} - u_{0j\beta}) = \frac{e}{\Omega} \sum_{j\beta} Z_{j\alpha\beta}^* \Delta u_{j\beta}, \quad (1)$$

where $\Delta u_{j\beta}$ is the displacement of ion j in Cartesian direction β, $Z_{j\alpha\beta}^*$ is its Born effective charge tensor, and Ω is the unit cell volume. The zero subscript generally refers to an insulating centrosymmetric reference structure (in this case, either cubic perovskite or $R\bar{3}c$). The spontaneous polarization is obtained from Eq. (1) by considering a specific structural (or *switching*) pathway parametrized by the change in atomic displacements connecting a centrosymmetric reference structure and $R3c$.

Table IV summarizes our calculated BECs for the three different structures studied in this work. The BECs are calculated by finite differences: the ions are displaced slightly along [111] from their equilibrium positions, and the resulting change in polarization is calculated using the Berry-phase method described in Sec. II. The displacements are chosen to be small enough to ensure the validity of the linear treatment in Eq. (1). (Typical displacements used here are of the order of 0.01Å.) For the LSDA+U calculations we use $U_{eff}=2$ eV, since this value gives an insulating solution for all systems. (Higher values of U_{eff} would result only in small quantitative changes.)

The highly anomalous values of the BECs computed in the cubic structure, and the reduction of these values after freezing in the structural distortions, are in agement with former observations in other ferroelectric materials.[40,45] In particular, the large values of the Bi BECs emphasize the important role of this ion as the driving force of the ferroelectric distortion.[7] This is in contrast to the Li ion in the

related compound LiNbO$_3$,[40] whose effective charge is found not to deviate appreciably from its nominal value.

In Table IV we also report the polarization difference between the cubic (or $R\bar{3}c$) centrosymmetric structures and $R3c$. Using Eq. (1) and the $R3c$ LSDA BECs, 84.2 μC/cm^2 is obtained along [111],[48] a value consistent with the large displacements and BECs. Yet since Eq. (1) is only valid for small displacements and because the BECs are found to change considerably along the path (compare the LSDA+U results for cubic, $R\bar{3}c$, and $R3c$ structures in Table IV), this value is only a rough estimate of the polarization in BiFeO$_3$. This can be clearly seen from the larger values of 123.1 and 101.2 μC/cm^2 for ΔP, also given in Table IV, obtained using the cubic perovskite and $R\bar{3}c$ BECs, respectively. The accuracy could be improved by breaking the path into shorter segments and recomputing the BECs at intermediate points on the path. However, it is more efficient to compute the polarization directly from the Berry-phase theory, as will be described in the next section.

2. Modern theory of polarization

An accurate quantitative method for computing the polarization to all orders in displacement is the so-called Berry-phase (or "modern") theory of polarization,[19–21] discussed in Sec. II. In this approach, the electronic contribution to the polarization is calculated as a geometric phase, formally equivalent to the sum of Wannier centers of the occupied bands (where each center is assigned a charge e).[19,20] Because of the Born–von Kármán periodic boundary conditions employed here, there is an ambiguity in the choice of unit cell and the total polarization may only be determined up to an integer multiple of the polarization quantum $e\mathbf{R}/\Omega$, where e is the charge of the electron, $\mathbf{R}$ is a lattice vector in the direction of polarization, and Ω is the volume of the unit cell.[19–21] Thus, for a given structure, the theory yields a *lattice* of values. The difference in polarization between two structures (e.g., a polar structure and its enantiomorph) is therefore determined only up to an integer multiple of the polarization quantum. To predict which of the values would be obtained in a Sawyer–Tower or CV experiment, it is also necessary to specify a switching path along which the system stays insulating in all intermediate structural states.[46]

In the case of BiFeO$_3$ the polarization lattice of the $R3c$ ground state is computed to be $(6.6+n184.2)$ μC/cm^2 along [111] within the LSDA, where n is an integer and $|e\mathbf{R}/\Omega|$ $=184.2$ μC/cm^2 is the polarization quantum along [111]. Similar results are obtained with LSDA+U (see Table V), though a small shift in polarization with increasing U_{eff} is observed. From the values in Table V it can be seen that this shift is mainly due to the effect of U_{eff} on the *electronic* structure whereas the corresponding *structural* change has only minor influence (although the structural influence is more pronounced for $U_{\text{eff}}=4$ eV). This reflects the fact that the use of a nonzero U_{eff} in this system leads to only small changes in the structure. Given the uncertainty in U_{eff} and relative similarity of these results, we focus on the $U_{\text{eff}}=0$ case in the discussion below. If the point $n=0$ is selected, near-perfect agreement is obtained with the measurement of

TABLE V. Minimum value of the polarization lattice (P_{min}), half the polarization quantum [$(1/2)|e\mathbf{R}/\Omega|$] along [111], and predicted spontaneous polarization (P_s), all given in units of μC/cm^2, for $R3c$ with different U_{eff}. Here, values of P_s assume a path through an $R\bar{3}c$ centrosymmetric phase. For the upper three rows the structure obtained for $U_{\text{eff}}=0$ eV is used when computing the polarization. For the last two rows the corresponding lattice parameters as given in Table II are used for each U_{eff}.

U_{eff} (eV)	P_{min}	$(1/2)|e\mathbf{R}/\Omega|$	P_s
0	6.6	92.1	98.7
2	2.6	92.1	94.7
4	1.2	92.1	93.3
2	2.4	91.6	94.0
4	−1.8	91.6	89.7

6.1 μC/cm^2 by Teague *et al.*[13] over 30 years ago. However, it is initially puzzling that none of the allowed values are at all close to the estimate of 84.2 μC/cm^2 made in the previous section, using Eq. (1) and based on paths involving nearby centrosymmetric structures.

This discrepancy is immediately resolved by computing the allowed values of the polarization *difference* between a centrosymmetric structure and $R3c$. In this case it turns out that the centrosymmetric $R\bar{3}c$ and cubic perovskite structures have a polarization not of zero (modulo the polarization quantum) but of half of a polarization quantum (92.1 $+n184.2$) μC/cm^2 along [111].[49] Thus one of the allowed values for the polarization difference between $R3c$ and the centrosymmetric reference structures, computed with the Berry-phase theory, is 98.7 μC/cm^2 ($U_{\text{eff}}=0$), agreeing well with the linear estimate of the previous section. That the centrosymmetric structure has a nonzero value of polarization may at first seem counterintuitive. However, it is readily understood using the Wannier function reformulation of the Berry-phase expression.[20] Making the conservative assumption that the Wannier functions are centered on atoms with
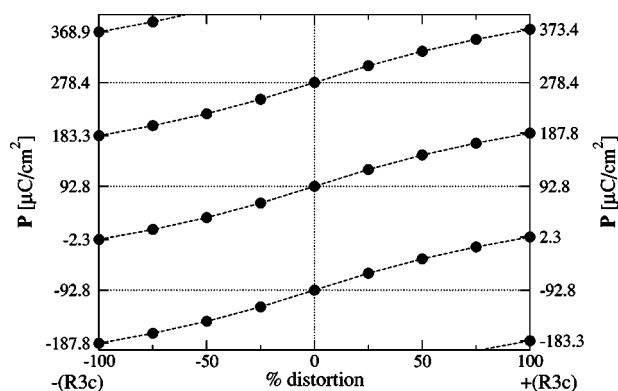

FIG. 5. Change in polarization **P** along a path from the original $R3c$ structure through the centrosymmetric cubic structure to the inverted $-(R3c)$ structure calculated with the LSDA+U method and $U_{\text{eff}}=2$ eV. The possible values of **P** for fixed distortion differ by multiples of the polarization quantum, here 185.6 μC/cm^2 for α $=60°$.

multiplicity consistent with formal valences of $+3$ for Bi and Fe and -2 for oxygen; taking the origin at a Bi atom; and choosing as the additional basis atoms the Fe in the center of the ideal cubic perovskite unit cell and the three oxygens at the centers of the faces, the Wannier sum yields a polarization of 92.1 μC/cm^2 along [111] for the doubled unit cell (using the $R3c$ volume). This value is exactly half of a polarization quantum, the only nonzero value allowed by symmetry for the centrosymmetric cubic perovskite and $R\bar{3}c$ structures,[20] and also exactly the same value that is obtained by the exact calculation of the polarization for both centrosymmetric structures (cubic perovskite and $R\bar{3}c$). Alternate choices of origin and basis could result in other points on the polarization lattice, all differing by a polarization quantum, but would never produce zero for these BECs.

To connect the allowed polarization difference of 98.7 μC/cm^2 to a specific path in structural space, we compute the polarization from the Berry-phase theory for the endpoints and several intermediate structures along an idealized "switching path" connecting the positively oriented $+(R3c)$ with its enantiomorphic counterpart, the negatively oriented $-(R3c)$ structure with opposite polarization, through the centrosymmetric cubic perovskite structure. Although the actual displacements associated with switching will obviously be more complex, the atomic positions are assumed to travel smoothly from positive to negative orientation through the cubic arrangement. Also, for simplicity these calculations assume a rhombohedral angle $\alpha = 60°$ for $R3c$ and the volume obtained within LSDA, which slightly shifts the polarization quantum to 185.5 μC/cm^2 and the Berry-phase polarizations by a few percent. Since the cubic perovskite structure is metallic within LSDA, we use results obtained for $U_{eff} = 2$ eV. The results are shown in Fig. 5. For the specific continuous insulating path connecting the $-(R3c)$ lattice point corresponding to -2.3 μC/cm^2 with the $+(R3c)$ point of 187.8 μC/cm^2, the polarization is seen to evolve smoothly (but nonlinearly) through the centrosymmetric cubic structure, which has a nonzero polarization. Subtracting the two end-point values gives a polarization change of 190.1 μC/cm^2 and a predicted spontaneous polarization of half that value, or 95.05 μC/cm^2. (The slight difference from the value of 98.7 μC/cm^2 reported above is due to the assumptions $\alpha = 60°$ and $U_{eff} = 2$ eV.) This value is consistent with measurements on (111) oriented thin films,[9] as well as our estimate with Eq. (1).

IV. DISCUSSION: POSSIBILITY OF MULTIPLE POLARIZATION PATHS

In the previous section we observed that if the system switches along the path indicated in Fig. 5 (or along one that can be continously deformed into it) the modern theory of polarization predicts a measured spontaneous polarization of $\sim 90-100$ μC/cm^2, depending on the choice of U_{eff}. In principle, however, an infinite set of polarization differences between the $+(R3c)$ and $-(R3c)$ structures is possible, provided that a suitable pathway can be found to connect any two end points. For example, if a switching path could be found taking $+(R3c)$ to $-(R3c)$ through an intermediate structure with

zero polarization, the measured polarization would be 2.3 μC/cm^2 (for $U_{eff} = 2$ eV), consistent with reports for bulk samples.[13] Thus although the possibility of the small experimental values resulting from poor sample quality cannot be ruled out, it is nonetheless interesting that different reported values for polarization (both lower, ≈ 6 μC/cm^2, and higher, >150 μC/cm^2) may be explained by different *switching paths*.

Specific paths connecting the smallest $+(R3c)$ polarization value with the smallest $-(R3c)$ value have yet to be determined. One approach to finding such a path would be to identify a centrosymmetric reference structure with zero polarization (modulo a quantum), the path then being the atomic displacements from $R3c$ to this structure. To get a zero (or integer-quantum) polarization from only a small distortion of the perovskite structure would require a somewhat drastic rearrangement of the centers of the Wannier functions. In the present case this may be facilitated by the known multiple valences possible for Bi and Fe. For example, if the Bi ions were to acquire an average formal charge of $+4$ (likely if a disproportionation to Bi^{3+} and Bi^{5+} occurred, leaving the Fe with a $+2$ charge), the polarization of the cubic phase would be zero. Further, by combining a forward switching path between $R3c$ enantiomorphs through an integer-polarization structure with another switching path back through a half-quantum-polarization structure (e.g., $R\bar{3}c$), the BiFeO$_3$ crystal could be taken to itself with a net transport of electrons across the system. This suggests the intriguing possibility of an insulating crystal with nonzero electronic conductivity.

In constructing paths corresponding to different polarizations, we do not wish to claim knowledge of the actual experimental switching mechanism, which is certainly much more complicated. In reality, switching is thought to occur via domain wall motion, where the key physics is associated with polarization reversal under an applied electric field at interfaces between positively and negatively oriented domain walls.[47]

Finally, an alternative explanation for the different polarizations reported in various film and bulk samples would be that different crystal structures are epitaxially stabilized in the films, which in turn possess significantly different polarizations. An alternative tetragonal structure that satisfied this requirement was discussed in a previous paper.[8] To clarify these issues further experimental work will be necessary to determine the sensitivity of the structure of thin film BiFeO$_3$ to substrate and growth orientation.

V. CONCLUSIONS

In summary, BiFeO$_3$ is a material of unusual interest both as a potentially useful multiferroic, and with respect to its fundamental polarization behavior. A wide range of measured polarization values have been reported, all of which are apparently permitted within the modern theory of polarization[19–21] by the lattice character of the polarization. Since some of the observed values of polarization can only be explained by switching through structures in which the ions change their valence states, such behavior, if experimen-

tally verified, might be unique to multiferroics, in which the magnetic transition metals are able to adopt multiple values for *d*-orbital occupancy.

*Present address: The Molecular Foundry, Materials Sciences Division, Lawrence Berkeley National Laboratory, Berkeley, CA 94720, USA.

[1] H. Ohno, Science **281**, 951 (1998).

[2] S. A. Wolf, D. D. Awschalom, R. A. Buhrman, J. M. D. S. von Molnár, M. L. Roukes, A. Y. Chtchelkanova, and D. M. Treger, Science **294**, 1488 (2001).

[3] G. A. Smolenskii and I. E. Chupis, Sov. Phys. Usp. **25**, 475 (1982).

[4] H. Schmid, Ferroelectrics **62**, 317 (1994).

[5] N. A. Hill, J. Phys. Chem. B **104**, 6694 (2000).

[6] B. B. van Aken, T. T. M. Palstra, A. Filippetti, and N. A. Spaldin, Nat. Mater. **3**, 164 (2004).

[7] R. Seshadri and N. A. Hill, Chem. Mater. **13**, 2892 (2001).

[8] J. Wang *et al.*, Science **299**, 1719 (2003).

[9] J. F. Li, J. Wang, N. Wang, F. Bai, B. Ruette, A. P. Pyatakov, M. Wuttig, R. Ramesh, A. K. Zvezdin, and D. Viehland, Appl. Phys. Lett. **84**, 5261 (2004).

[10] K. Y. Yun, D. Ricinschi, T. Kanashima, M. Noda, and M. Okuyama, Jpn. J. Appl. Phys., Part 2 **43**, L647 (2004).

[11] C. Michel, J.-M. Moreau, G. D. Achenbach, R. Gerson, and W. J. James, Solid State Commun. **7**, 701 (1969).

[12] F. Kubel and H. Schmid, Acta Crystallogr., Sect. B: Struct. Sci. **46**, 698 (1990).

[13] J. R. Teague, R. Gerson, and W. J. James, Solid State Commun. **8**, 1073 (1970).

[14] J. Íñiguez, L. Bellaiche and D. Vanderbilt, Phys. Rev. B **67**, 224107 (2003).

[15] K. Ueda, H. Tabata, and T. Kawai, Appl. Phys. Lett. **75**, 555 (1999).

[16] V. R. Palkar, J. John, and R. Pinto, Appl. Phys. Lett. **80**, 1628 (2002).

[17] Y. P. Wang, L. Zhou, M. F. Zhang, X. Y. Cheng, J.-M. Liu, and Z. G. Liu, Appl. Phys. Lett. **84**, 1731 (2004).

[18] K. Y. Yun, M. Noda, and M. O. Kuyama, Appl. Phys. Lett. **83**, 3981 (2003).

[19] R. D. King-Smith and D. Vanderbilt, Phys. Rev. B **47**, 1651 (1993).

[20] D. Vanderbilt and R. D. King-Smith, Phys. Rev. B **48**, 4442 (1994).

[21] R. Resta, Rev. Mod. Phys. **66**, 899 (1994).

[22] C. Ederer and N. A. Spaldin, cond-mat/0407003, Phys. Rev. B (to be published).

[23] P. Hohenberg and W. Kohn, Phys. Rev. **136**, B864 (1964).

[24] W. Kohn and L. J. Sham, Phys. Rev. **140**, A1133 (1965).

[25] V. I. Anisimov, F. Aryasetiawan, and A. I. Liechtenstein, J. Phys.: Condens. Matter **9**, 767 (1997).

[26] G. Kresse and J. Hafner, Phys. Rev. B **47**, R558 (1993).

[27] G. Kresse and J. Furthmüller, Phys. Rev. B **54**, 11 169 (1996).

[28] P. Blöchl, Phys. Rev. B **50**, 17 953 (1994).

[29] G. Kresse and D. Joubert, Phys. Rev. B **59**, 1758 (1999).

[30] C. Elsässer, M. Fähnle, C. T. Chan, and K. M. Ho, Phys. Rev. B **49**, 13 975 (1994).

[31] H. J. Monkhorst and J. D. Pack, Phys. Rev. B **13**, 5188 (1976).

[32] K. Terakura, T. Oguchi, A. R. Williams, and J. Kübler, Phys. Rev. B **30**, 4734 (1984).

[33] S. L. Dudarev, G. A. Botton, S. Y. Savrasov, C. J. Humphreys, and A. P. Sutton, Phys. Rev. B **57**, 1505 (1998).

[34] P. E. Blöchl, O. Jepsen, and O. K. Andersen, Phys. Rev. B **49**, 16 223 (1994).

[35] A. Rohrbach, J. Hafner, and G. Kresse, J. Phys.: Condens. Matter **15**, 979 (2003).

[36] G. Rollmann, A. Rohrbach, P. Entel, and J. Hafner, Phys. Rev. B **69**, 165107 (2004).

[37] I. Sosnowska, T. Peterlin-Neumaier, and E. Steichele, J. Phys. C **15**, 4835 (1982).

[38] G. P. Vorob'ev, A. K. Zvezdin, A. M. Kadomtseva, Y. F. Popov, V. A. Murashov, and D. N. Rakov, Phys. Solid State **37**, 1793 (1995).

[39] I. Inbar and R. E. Cohen, Phys. Rev. B **53**, 1193 (1996).

[40] M. Veithen and P. Ghosez, Phys. Rev. B **65**, 214302 (2002).

[41] C. J. Bradley and A. P. Cracknell, *The Mathematical Theory of Symmetry in Solids* (Oxford University Press, Oxford, 1972).

[42] I. Sosnowska, W. Schäfer, W. Kockelmann, K. H. Andersen, and I. O. Troyanchuk, Appl. Phys. A: Mater. Sci. Process. **74**, S1040 (2002).

[43] V. I. Anisimov, I. S. Elfimov, N. Hamada, and K. Terakura, Phys. Rev. B **54**, 4387 (1996).

[44] V. I. Anisimov and O. Gunnarsson, Phys. Rev. B **43**, 7570 (1991).

[45] P. Ghosez, J.-P. Michenaud, and X. Gonze, Phys. Rev. B **58**, 6224 (1998).

[46] U. V. Waghmare, Ph.D. thesis, Yale University, 1996.

[47] A. Tagantsev, I. Stolichnov, E. Colla, and N. Setter, J. Appl. Phys. **90**, 1387 (2001).

[48] The inversion symmetry-breaking displacements along [111] from cubic perovskite to $R3c$ are the same as those from $R\bar{3}c$ to $R3c$.

[49] Here we assume the volume of the centrosymmetric structure is equal to that of $R3c$. In general this will not be the case (see Table III for $R\bar{3}c$), and the polarization quantum will differ for the two structures. When computing the spontaneous polarization, this discrepancy can be avoided by taking differences between two end-point phases, as is done throughout this work.